Empirical Formula of Exciton Coherent Domain in Oligomers and Application to LH2†

Toshiaki Kakitani* and Akihiro Kimura

Department of Physics, Graduate School of Science, Nagoya University, Chikusa-ku, Nagoya 464-8602, Japan, and Graduate School of Human Informatics, Nagoya University, Chikusa-ku, Nagoya 464-8601, Japan

Received: July 3, 2001; In Final Form: November 20, 2001

We investigated the mechanism by which the length of exciton coherent domain in the linear array of pigments is determined. Correctly solving a generalized master equation with memory function obtained by the second-order perturbation of the intermolecular interaction, we obtained an empirical formula for the length of exciton coherent domain, abbreviated as coherence length. In the absence of inhomogeneity, this coherence length is expressed by a linear function of the ratio between the intermolecular coupling strength U and the destructing force γ of a coherent bond. In the presence of inhomogeneity, the coherence length is expressed by a linear function of U/γ only approximately, and its deviation becomes significant when the degree of inhomogeneity is larger than about 100 cm^{-1}. Applying this formula to the LH2 antenna complex of photosynthetic purple bacteria *Rhodopseudomonas acidophila*, we found that the coherence length of B850 is about 5 bacteriochlorophyll molecules in the absence of inhomogeneity and about 4 in the presence of inhomogeneity. The coherence length of B800 is less than 1.6, confirming that the excited state of B800 is almost localized at one bacteriochlorophyll molecule.

1. Introduction

Excitation energy transfer (EET) is a significant process in physics, chemistry, and biology. Especially the EET in the antenna complex of photosynthetic systems plays a central role in photoenergy conversion.[1,2] Recently, a considerable number of three-dimensional structures of antenna complexes are clarified by the X-ray crystallographycal and electrodiffraction analyses.[3−9] Those structures represent much variety of arrangements of pigments. Therefore, we are now ready to study the detailed EET mechanism on the basis of rigid molecular arrangements.

Among the structure-solved antenna systems, the light-harvesting antenna system 2 (LH2) in photosynthetic purple bacteria *Rhodopseudomonas* (*Rps.*) *acidophila* and *Rhodospirillum* (*Rs.*) *molischianum* are nonameric circular aggregates of α,β-heterodimers, with each subunit noncovalently binding three bacteriochlorophylls (BChl). In LH2 of *Rps. acidophila*, 18 and 9 BChls are arranged in rings which absorb light of 850 and 800 nm wavelength, called B850 and B800, respectively. The transition dipole−dipole interaction which is called intermolecular interaction hereafter is large ($\sim$300 cm^{-1})[10] in B850 and is small ($\sim$20 cm^{-1})[10] in B800. The intermolecular interaction between B800 and B850 is also small ($\sim$20 cm^{-1}).[10]

Under these situations, it was very often assumed that the exciton state exists in B850 is completely delocalized and the excited state in B800 is completely localized.[11−13] Furthermore, it was often assumed that the excitation transfer from B800 to B850 is due to the Förster mechanism from the completely localized state of B800 to the completely delocalized state of B850.[12−14] A different version of the Förster model using the forbidden state of exciton which becomes available when molecular size is so large that it is comparable with the donor and acceptor distance was also applied to this system.[15,16] The latter model succeeded in reproducing the experimentally observed very fast EET (in 0.7 ps) from B800 to B850.[17]

We should be reminded of the fact that in many calculations they assumed completely delocalized exciton states for B850 and completely localized states for B800 because the intermolecular coupling in B850 is about 1 order of magnitude larger than that in B800. However, we should remember that the EET mechanism changes depending on the degree of coherency of the excited state. Namely, we should carefully examine the length of exciton coherent domain, which we call coherence length hereafter. Indeed, there are some experimental data of the pump−probe spectroscopy suggesting that the coherence length extends over only several units in B850 at room temperature.[18,19] There is also experimental data that the magnitude of superradiance of B850 at room temperature is as small as 2.8.[20] From the aspect of theoretical study, Kühn and Sundström[21] evaluated the coherence length of B850 in the presence of inhomogeneity as around 4 with use of the Redfield theory.[22] Ray and Makri[23] investigated the coherence length of B850 by the path integral theory and estimated it as about 2 either in the presence or absence of inhomogeneity at room temperature. Therefore, the determination of the coherence length of B850 is very important and it is a problem of much debate up to the present time.[21−26]

Under such situation, we formerly constructed a dimer theory applicable to the intermediate coupling case which is the interpolation of the exciton theory in the strong coupling case and the Förster theory in the weak coupling case.[27,28] We derived formulas of criteria which classify EET mechanisms into three classes: exciton mechanism, intermediate coupling mechanism, and Förster mechanism.[28] We also derived a new formula for evaluating the degree of coherency for all the coupling strength.[28] The EET due to the intermediate coupling mechanism applies when donor or acceptor has incomplete coherency in the excited state or when EET takes place on the way of

† Part of the special issue "Noboru Mataga Festschrift".

* Corresponding author. Tel. and Fax: +81-52-789-3528. E-mail: kakitani@allegro.phys.nagoya-u.ac.jp.

10.1021/jp012516q CCC: $22.00
Published on Web 02/12/2002

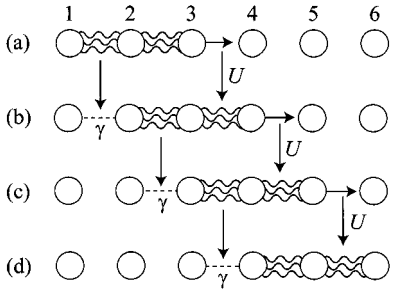

Figure 1. Schematic representation of formation and destruction of a coherent bond at the end of exciton coherent domain in the steady state. The coherent bond is represented by triple wavy lines. The coherent bond to be produced is represented by a solid arrow, and the broken coherent bond is represented by a broken line. Stages of the exciton coherent domain for each lapse of unit time ($= T_F$) are represented from (a) to (d). The transition of the stage (a) to the stage (b) takes place by breaking the coherent bond 1−2 and forming a coherent bond 3−4, and so on. During the transitions from (a) to (d), the coherent bonds 2−3, 3−4, and 4−5 are maintained for two unit times. This fact indicates that the destruction time T_D is equal to $2T_F$. Therefore, using eq 1 in the text, we obtain $N_{coh} = 3$, which agrees with the picture of exciton coherent domain drawn as a trimer.

vibrational relaxation in the donor excited state. We could show that the range of the intermolecular coupling strength which applies to the intermediate coupling case definitely exists, and in reality its range is considerably large, depending on the magnitude of electron−phonon interaction.

In the present paper, using this dimer theory, we obtain an empirical formula for easily evaluating the coherence length N_{coh} of the excitonic state of oligomer in a linear array of pigments. Before going into its detail, we first show a basic concept of this formula in the following.

Let us now assume that the intermolecular coupling U is a force which works to produce coherent excitonic coupling between the neighboring pigments which we call coherent bond hereafter. The time T_F for formation of a coherent bond is $T_F \simeq h/4U$ which is a half period of the oscillation of the excited state between two molecules. On the other hand, thermal fluctuations due to the electron−phonon interaction works to destruct the coherent bond. This is usually called dynamical effect. So, let us assume that the exponentially decay constant γ of the two-time correlation function of the intermolecular interaction[28] is the destruction force of a coherent exciton bond. The time T_D necessary for destructing the coherent bond is estimated as about $\hbar/\gamma$ on the basis of an uncertainty principle. The validity of these assumptions are proved in the latter section.

The competition between formation of a coherent bond and destruction of the coherent bond takes place. These situations are schematically drawn in Figure 1, where the case is written that a coherent region is elongated by one at the right end and the coherent region is shortened at the left end for each step. Actually, the elongation and destruction of coherent bonds will take place stochastically. In such a way, the length of the coherent region converges and the exciton coherent domain moves in the steady state. Its average coherence length N_{coh} is estimated as

$$N_{coh} = \frac{T_D}{T_F} + 1 \simeq 1.57\frac{U}{\gamma} + 1 \tag{1}$$

where we added 1 in order to set $N_{coh} = 1$ in the case of $U = 0$. In Figure 1, T_D and T_F are chosen as 1 and 2 steps of transition, and we obtain $N_{coh} = 3$.

On the basis of such qualitative consideration, we expect that the coherence length N_{coh} will be expressed by a linear function of the ratio U/γ. In the following sections, we shall show that this really happens by quantitative calculations.

2. Intermediate Coupling Theory of Dimer

To obtain the coherence length in oligomers, we make use of the concept of degree of coherency which was developed in the dimer theory. For this purpose, we shortly review the dimer theory in this section. This dimer theory was based on the three state model: ground state of the donor D plus a photon $h\nu$ to be absorbed (d state), the excited state of donor D* (m state), and the excited state of acceptor A* (a state). At time $t = 0$, a short pulse light irradiation is made to D, producing D* at the Franck−Condon state. We solve the Liouville equation of density operator nonperturbatically. For this purpose, we introduced a method of factorization using a two-time correlation function and adopted an exponential form of the correlation function. In the case that the vibrational relaxation time τ_r is much larger than EET time, we obtain a probability $n_a(t)$ that the acceptor is excited as follows:

$$n_a(t) = 1 - e^{-\gamma t/\hbar}\left[\cosh\sqrt{\alpha}t + \frac{\gamma}{2\hbar\sqrt{\alpha}}\sinh\sqrt{\alpha}t\right]^2 \tag{2}$$

where

$$\alpha = \left(\frac{\gamma}{2\hbar}\right)^2 - \left(\frac{U}{\hbar}\right)^2 \tag{3}$$

$$\gamma = \frac{1}{\pi(FC)_0} = \frac{1}{\pi}\sqrt{4\pi(\lambda_m + \lambda_a)k_BT'}\exp\left\{\frac{(\Delta G_{am} + \lambda_a - \lambda_m)^2}{4(\lambda_m + \lambda_a)k_BT'}\right\} \tag{4}$$

$$k_BT' = \frac{1}{2}\hbar\bar{\omega}\coth\left(\frac{\hbar\bar{\omega}}{2k_BT}\right) \tag{5}$$

In the above equations, λ_m and λ_a are the reorganization energies due to the excitation of donor and acceptor, respectively, $\bar{\omega}$ is an average angular frequency of vibration, and ΔG_{am} is the free energy difference between the a state and m state in equilibrium condition. The decay factor γ is defined as the inverse of the Franck−Condon factor for exciton transfer which was tentatively expressed by the Gaussian form. As we see later, this decay factor is equal to the destructing force of the coherent bond.

In the above equations, U and γ mostly appear in a combined form of U/γ. So, we define a new parameter ξ as follows:

$$\xi = \frac{2U}{\gamma} \tag{6}$$

When $\xi > 1$ holds, α becomes negative and $n_a(t)$ is a function of the damped oscillation of time, expressing the property of exciton or partial exciton. When $\xi < 1$ holds, α becomes positive and $n_a(t)$ is overdamped with time, expressing nonexcitonic behavior.

The frequency ν of damped oscillation in the case $\xi > 1$ is written as

$$h\nu = \frac{h}{\pi}\sqrt{|\alpha|} = \sqrt{4U^2 - \gamma^2} = \gamma\sqrt{\xi^2 - 1} \tag{7}$$

The split of the two exciton levels corresponds to $h\nu$ and it decreases as ξ is decreased, finally becoming zero at $\xi = 1$. Namely, the excitonic character disappears for $\xi \leq 1$.

Using $n_a(t)$, we defined the EET rate which applies to all the values of U as follows:[28]

$$k_{ad}^{max} = \left|\frac{dn_a(t)}{dt}\right|_{t=t_{max}} \quad (8)$$

where t_{max} indicates the time when $dn_a(t)/dt$ becomes maximum. In this definition, k_{ad}^{max} becomes proportional to U in the extremely strong coupling case (exciton case), in agreement with the formal velocity as proposed by Förster.[29] Similarly, k_{ad}^{max} becomes proportional to U^2 in the extremely weak coupling case, in agreement with the Förster mechanism.[30] In the intermediate case,

$$k_{ad}^{max} \propto U^x \ (1 < x < 2) \quad (9)$$

holds. It is reasonable to define the degree of coherency to be 0 for $x = 2$ and 1 for $x = 1$. Considering this, we defined the degree of coherence η as[28]

$$\eta = 2 - x \quad (10)$$

In other words, we defined η as

$$\eta = 2 - \frac{\partial \ln k_{ad}^{max}}{\partial \ln U} \quad (11)$$

We should remember that there exists a critical point of η at η_c[28]

$$\eta_c = 1 - \sqrt{2}/3 = 0.528595\cdots \quad (12)$$

where $\xi = 1$ holds. When η is larger than η_c, the oscillation of $n_a(t)$ remains, but it disappears when η is less than η_c. Then, we can use η_c as a threshold that excitonic character is retained for $\eta \geq \eta_c$.

Before closing this section, we emphasize that the concept of the degree of coherency is usable for all the values of ξ so far as we solve the Liouville equation self-consistently, even if we adopted a method of factorization by a two-time correlation function.

3. Generalized Master Equation

To extend the dimer theory to the oligomer case, we make use of the generalized master equation (GME). The probability $P_a(t)$ that the molecule at site a is excited is written as

$$\frac{dP_a(t)}{dt} = \sum_{b \neq a} \int_0^t dt_1 [M_{ab}(t, t_1)P_b(t_1) - M_{ba}(t, t_1)P_a(t_1)] \quad (13)$$

where $M_{ab}(t, t_1)$ is the memory function for the EET from the excited state of molecule a to the excited state of molecule b. We adopt the second-order perturbation of the intermolecular coupling for evaluating the memory function. In this case, the memory function only for the neighboring molecules becomes nonzero. We apply an intermediate coarse graining. We assume Lorentzian shape of optical absorption and emission spectra for each molecule. This would be appropriate when we investigate the coherency in the time region close to the steady state. Then, we can derive the following formula of memory function:[31]

$$M_{ab}(t, t_1) = \frac{2U_{ab}^2}{\hbar^2}\cos(\Delta G_{ab}(\tau)\mu/\hbar) \exp[-\gamma_{ab}\mu/\hbar] \quad (14)$$

with $\tau = (t + t_1)/2$ and $\mu = t - t_1$. In eq 14, $\Delta G_{ab}(\tau)$ is the energy gap for the EET at time τ after molecule a is excited to the Franck−Condon state of molecule a and is given as follows:[28]

$$\Delta G_{ab}(\tau) = \Delta G_{ab} + \lambda_a + \lambda_b - 2\lambda_a(\tau) \quad (15)$$

$$\lambda_a(\tau) = \lambda_a e^{-\tau^2/\tau_v^2} \quad (16)$$

where τ_v is the vibrational relaxation time. The parameter γ_{ab} is the decay factor expressed as

$$\gamma_{ab} = \Gamma_a^f + \Gamma_b^a \quad (17)$$

where Γ_a^f and Γ_b^a are the half width of the half-maximum (HWHM) of the intrinsic emission spectrum of donor and the intrinsic absorption spectrum of acceptor, respectively.

When the energy gap is small or negligible, eq 14 can be written as

$$M_{ab}(t, t_1) = \frac{2U_{ab}^2}{\hbar^2} \exp\left[-\frac{\gamma_{ab}}{\hbar}\mu\right] \quad (18)$$

The form of eq 4 is the same as used in the two-time correlation function in the dimer theory of ref 28.

Such form of $M_{ab}(t, t_1)$ as eq 14 is correct in the weak coupling case. Furthermore, within this theoretical framework we obtain an exact exciton solution corresponding to the limit of strong coupling case ($\xi = \infty$), as proved by Kenkre and Knox.[32] Then, it will be still usable approximately in the intermediate coupling case if we solve the GME rigidly using this memory function. This philosophy is the same as the case of dimer theory. In the dimer theory, we used the correlation function which is appropriate in the second-order perturbation of the intermolecular interaction and we solved the Liouville equation self-consistently (nonperturbatively).[28] After such treatment, we showed that the obtained EET theory is the interpolation from the exact theory in the weak coupling limit and from the exact theory in the strong coupling limit. In the same way, we solve the GME correctly using the memory function obtained by the second-order perturbation. Then, the calculated result can be the interpolation from the weak coupling case and from the strong coupling case.

4. Numerical Calculations

4.1. Homogeneous Case. We consider a molecular system in which the same molecules are arranged in a line with the same distance as shown in the inset of Figure 2. Molecules are numbered in an order of molecules. The initial state is the excitation of the end molecule (No. 1). We solve GME correctly by numerical calculations with use of the memory function of eq 14. The probability of the excited state at each molecule at time t is plotted in Figure 2. Here, the parameter values are chosen as $U = 350\ cm^{-1}$, $\gamma = 140\ cm^{-1}$, $\lambda_a = \lambda_b = 40\ cm^{-1}$ and $\tau_d = 1 \times 10^{-12}$ s. We dropped suffix ab from U and γ for simplicity because they are the same for all the neighboring molecules in this case. We see a successive transfer of excitation energy together with oscillation of the population.

Next, we calculate the degree of coherency η_n of the molecule at site n ($n \geq 2$) using the following equation

$$\eta_n = 2 - \frac{\partial \ln k_n^{max}}{\partial \ln U} \quad (19)$$

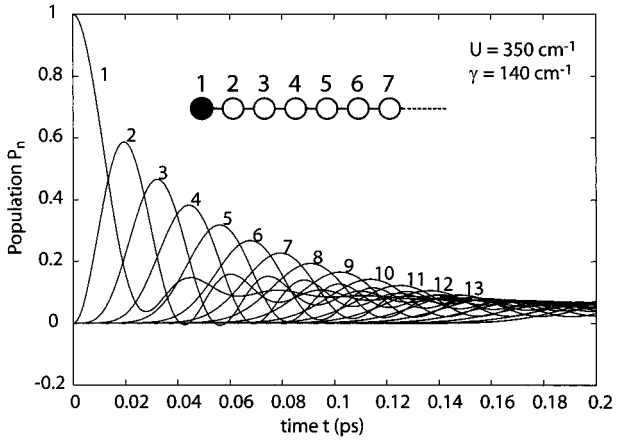

Figure 2. Time course of the probability P_n that the nth molecule is excited. Initially the end molecule (No. 1) is excited in the linear array of molecules. The used parameter values are $U = 350$ cm^{-1} and $\gamma = 140$ cm^{-1}.

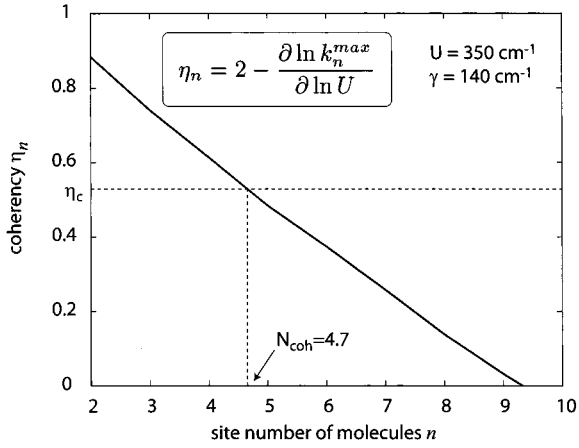

Figure 3. Calculated coherency η_n for each nth molecule. η_n is calculated by the equation written in the inset. The parameter values are $U = 350$ cm^{-1} and $\gamma = 140$ cm^{-1}.

with

$$k_n^{\max} = \left|\frac{dP_n(t)}{dt}\right|_{t=t_{\max}} \tag{20}$$

The derivative in eq 19 is obtained by calculating the change of $k_n^{\max}$ when U is changed a little from 350 cm^{-1}. The calculated result of η_n for the various values of n is shown in Figure 3. We see that η_n is a monotonically decreasing function of n. We search the site number of molecules where η_n becomes equal to η_c. The site number so obtained is the coherence length N_{coh} of EET. In this case $N_{\text{coh}} = 4.7$.

We do such calculations by varying the set of U and γ. First, we varied U from 100 cm^{-1} to 500 cm^{-1} by fixing γ at 140 cm^{-1}. The coherence length N_{coh} determined for each value of U is plotted in Figure 4. The signal + is the calculated point. We find that the calculated data are almost exactly on a line

$$N_{\text{coh}} = 1.38 + 1.33\frac{U}{\gamma}$$
$$= 1.38 + 0.67\xi \tag{21}$$

Next, we varied γ from 100 cm^{-1} to 500 cm^{-1} by fixing U at 350 cm^{-1}. Then, we obtained Figure 5. We find that the calculated data are almost exactly on a line

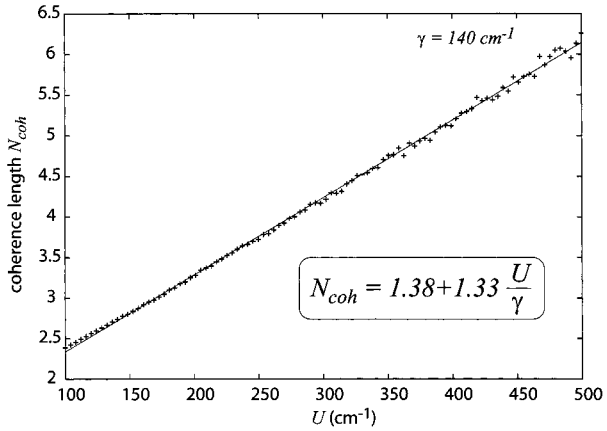

Figure 4. Correlation of the coherence length N_{coh} with the coupling strength U. The destructing force γ is fixed at 140 cm^{-1}. The numerically calculated points are represented by signal +. The best fit line is shown by the straight line. The empirical formula so obtained is written in the inset.

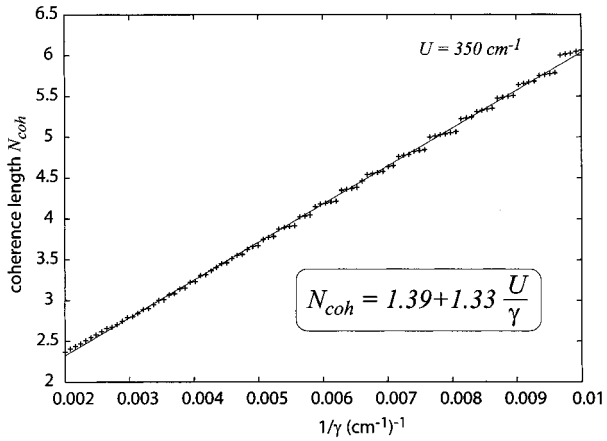

Figure 5. Correlation of the coherence length N_{coh} with the destructing force γ. The intermolecular coupling strength U is fixed at 350 cm^{-1}. The numerically calculated points are represented by signal +. The best best fit line is shown by the straight line. The empirical formula so obtained is written in the inset.

$$N_{\text{coh}} = 1.39 + 1.33\frac{U}{\gamma}$$
$$= 1.39 + 0.67\xi \tag{22}$$

Equation 22 is almost the same as eq 21. Namely, we obtained a very simple formula of the coherence length N_{coh} as a function of ξ. It should be mentioned that our obtained relation (eq 21 or 22) qualitatively coincides with the relation of eq 1, which was obtained by intuitive consideration. Therefore, we confirm that the coupling strength U works as coherent-bond-formation force and the decay constant γ works as coherent-bond-destruction force.

In eq 22, N_{coh} becomes 2.06 when $\xi = 1$. This result mostly agrees with the result of the dimer theory[28] that the $\eta = \eta_c$ happens at $\xi = 1$ for dimer, indicating that N_{coh} becomes 2 for $\xi = 1$. On the other hand, N_{coh} calculated from eq 22 for $\xi = 0$ becomes 1.39. Apparently this result indicates that there remains some coherency even at $U = 0$. Strictly speaking, this is unreasonable. But, its value is small enough to conclude that the excitation is localized.

In the above calculations, we assumed a linear array of molecules. When the molecules are arranged in large circle, there is no end molecule. In this case, we put the initial condition as the two neighboring molecules being excited half by half. Then,

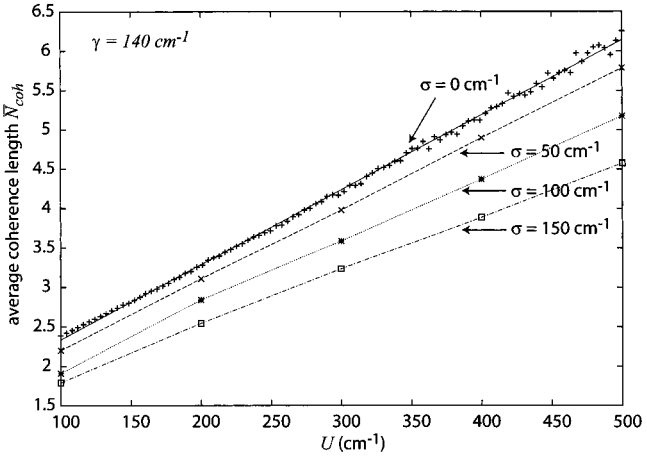

Figure 6. Correlation of the average coherence length $\bar{N}_{coh}$ with the coupling strength U for the four kinds of the inhomogeneous broadening width σ. The value of γ is fixed at 140 cm^{-1}.

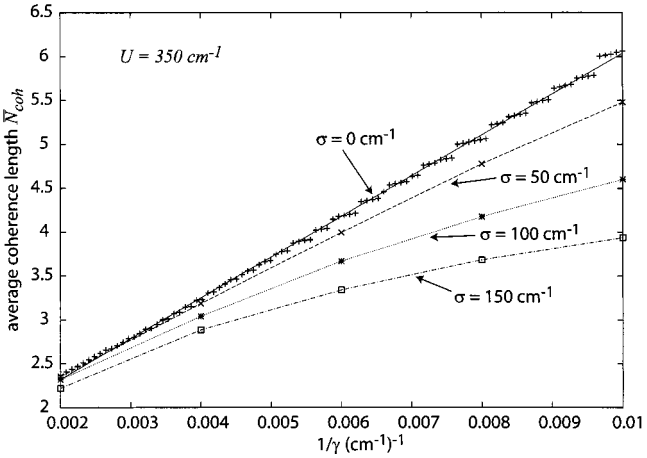

Figure 7. Correlation of the average coherence length $\bar{N}_{coh}$ with the destructing force γ for the four kinds of the inhomogeneous broadening width σ. The value of U is fixed at 350 cm^{-1}.

the EET proceeds in both directions. In one direction, the excited state of probability 0.5 propagates in both directions in the same way as the end molecule being excited initially in the linear array of molecules. The coherence length N_{coh} measured from the initially excited state is found to be the same as that of the linear array system considered above. Therefore, the same formula as eq 21 or eq 22 holds for the cyclic array of molecules, so far as the cyclic array is large enough so that the coherent regions progressed from both sides do not collide with each other.

4.2. Inhomogeneous Case. Now we consider the case that the energy gap ΔG_{ab} between the neighboring molecules distributes with a Gaussian form

$$f(\Delta G_{ab}) = \frac{1}{\sqrt{2\pi\sigma^2}} \exp\left[-\frac{(\Delta G_{ab})^2}{2\sigma^2}\right] \qquad (23)$$

where σ is the standard deviation. We calculate N_{coh} for each ΔG_{ab} using eq 14 as before. Then, we obtain the averaged coherence length $\bar{N}_{coh}$ as

$$\bar{N}_{coh} = \int_{-\infty}^{\infty} f(\Delta G_{ab}) N_{coh}(\Delta G_{ab})\, d(\Delta G_{ab}) \qquad (24)$$

In the actual calculation, we randomly sample 100 kinds of ΔG_{ab} following the distribution of eq 23. We have chosen σ as 0, 50, 100, and 150 cm^{-1}. The calculated results of $\bar{N}_{coh}$ as a function of U for the four kinds of σ are plotted in Figure 6. The value of γ is fixed to 140 cm^{-1}. We find that $\bar{N}_{coh}$ is well expressed by a linear function of U, the slope of which decreases with increase of σ.

The calculated results of $\bar{N}_{coh}$ as a function of $1/\gamma$ for the four kinds of σ are plotted in Figure 7. The value of U is fixed to 350 cm^{-1}. We find that the increase of $\bar{N}_{coh}$ with increase of $1/\gamma$ becomes a little dull as $1/\gamma$ becomes large. This tendency becomes remarkable as σ becomes large. Namely, the $1/\gamma$ dependence of $\bar{N}_{coh}$ deviates a little from a linear function for larger values of σ. Combining the results of Figure 6 and Figure 7, we should say that $\bar{N}_{coh}$ is expressed by a linear function of $U/\hbar$ only approximately and the deviation from a linear relation becomes significant when σ becomes larger than about 100 cm^{-1}.

4.3. Application to LH2. Let us calculate the coherence length of the B850 ring of LH2. On the basis of the appropriate parameter values which are surveyed by Sundström et al.,[10] we first choose U = 350 cm^{-1} and γ = 140 cm^{-1}. In the homogeneous case, we obtain N_{coh} = 4.7 from eq 22. In the inhomogeneous cases with σ = 100 cm^{-1} and 150 cm^{-1}, we obtain $\bar{N}_{coh}$ = 4.0 and 3.6, respectively, from Figure 6. Next, we choose the other values U = 300 cm^{-1} and γ = 100 cm^{-1}. Then, we obtain N_{coh} = 5.4 in the homogeneous case and we obtain $\bar{N}_{coh}$ = 4.6 and 4.1 for σ = 100 cm^{-1} and 150 cm^{-1}, respectively.

Therefore, the coherence length of B850 in the absence of inhomogeneity would be around 5. When we incorporate the inhomogeneity effect, the average coherence length would be around 4.

The parameter values U = 20 cm^{-1} and γ = 140 cm^{-1} for B800 are supposed to be one of typical ones.[10] From the formula of eq 22, we obtain N_{coh} = 1.6. When we use parameter values U = 20 cm^{-1} and γ = 100 cm^{-1}, we obtain N_{coh} = 1.7. In both cases, N_{coh} is less than 2.0. This value becomes smaller when we incorporate the inhomogeneous effect. So, we can say that the excited state of B800 is almost localized to one bacteriochlorophyll.

5. Discussion

The present method for evaluating the coherence length of EET is quite new. The prominent feature of this method is to use the degree of coherency which varies greatly in the intermediate coupling case. It should be stressed that the criteria among the strong coupling, intermediate coupling, and weak coupling cases are not determined by only the strength the interatomic coupling U but also by the destructing force γ.[28] We have shown more specifically that the coherence length is determined by the ratio U/γ. At the bond where the exciton coherent domain ends, the degree of coherence is close to η_c. We should remember that the excitonic bond with $\eta \sim \eta_c$ is just the central part of the intermediate coupling case.[28] Therefore, the EET theory of the intermediate coupling case played a vital role in deriving the empirical formula of coherence length.

In our calculations, initially an end molecule was excited and the exciton coherent domain is extended by the successive EET. We evaluated the coherence length by calculating the degree of coherency of each molecule successively from the end molecule and searched the molecule whose degree of coherence η becomes close to η_c for the first time. Therefore, one may think that the coherence length which we obtained is smaller than that in the steady state. However, this is not the case. As we discussed in the Introduction, we showed that N_{coh} can be

expressed as a linear function of $\xi(\equiv 2U/\gamma)$ in the steady state. In our above numerical calculations, we have seen that N_{coh} is indeed expressed by a linear function of ξ (eqs 21 and 22). This coincidence indicates that the coherence length which we calculate from the empirical formula corresponds to that in the steady state.

In contrast to the present method, many of the previous studies[21,25,26,33−39] on the excited state of oligomers were mostly based on the Redfield theory[22] which was obtained by the second-order perturbation treatment of the electron−phonon interaction. Therefore, this theory is applicable when the electron−phonon interaction is relatively weak, or in other words, the intermolecular interaction is strong. If the system starts from the complete exciton state by absorbing a photon, the exciton coherent domain gradually shrinks with time until the coherent length of the steady state.[21,39]

In evaluating the coherence length in previous theories, many kinds of definitions were used so far.[21,39] Among them, the correlation of nondiagonal matrix element of density function[21] is suitable to pick up the dynamical effect of the environmental perturbation. In contrast to this, the calculation of the participation ratio reflects at most the effect of static disorder. The definition of coherence length by the path integral method[23] is elegant. But its value is apt to be smaller than the correct value by about $\sqrt{3}$ times, as exemplified in the calculation of the coherent length of B850 in the complete exciton state ($\gamma = 0$).[23] Compared with these methods, our implemented method is based on the different physical picture. In our method of evaluating the degree of coherency, we first calculate the rate of EET which actually takes place and then we evaluate its U-dependence, we compare EETs of many systems with a little different values of U. So, this method theoretically makes use of many EET processes, and picks up the coherent part by comparison.

The coherence length of B850 in LH2 in the steady state evaluated with use of Redfield theory including the inhomogeneity effects is mostly around 4.[21,39] Our calculated value without the inhomogeneity is around 5, and the calculated value in the presence of inhomogeneity is around 4. Since the used parameter values might be somewhat different, direct comparison is not possible. But, it can be said that our result qualitatively agrees with the result obtained by the method of Redfield theory. This fact is significant by the following reason. In our theory, we start from the weaker intermolecular coupling case although its theory is correct in the strong coupling limit again. In contrast to this, the Redfield theory is basically reliable at the stronger intermolecular coupling case. We found that the two theories gave similar results for the coherence length of B850. So, it is possible to use both theories by comparison or in a complementary way for the other systems also. In our theory, we obtained an empirical formula of N_{coh} for the first time. Its formula is useful for easily estimating the coherence length for any given systems.

Recently, it was pointed out that the coherence length can change, depending on the time of probe after excitation and so it changes by the probing method.[39] This is a quite reasonable thing. In the following, we qualitatively examine how coherence length can be changed with time and is affected by the molecular environment. When the whole system is illuminated by light, all the molecules with intermolecular couplings go into a mixed state between the ground and excited state at short time and look for mutually nice phases of transition dipole moments to absorb an illuminated light energy. The time necessary for this phase recognition will be about $T_F(\equiv h/4U)$. The light absorption time T_L is estimated as about $\hbar/\gamma_0$ where γ_0 is the homogeneous line width of optical absorption (γ_0 is approximately expressed as $\sqrt{2\lambda_a k_B T}$). If $T_F < T_L$ holds, the exciton state which extends over the whole molecules with intermolecular couplings become ready to absorb a photon. However, we must also take care of the fact that the coherence-destructing force takes part in such a process due to the electron−phonon interaction. Let us assume for simplicity that it works in the mixed state in the same way as after photoabsorption where it works with a time constant of $T_D(\equiv\hbar/\gamma)$. It mostly happens that T_D is smaller than T_L as we can see from eq 4. Therefore, we can classify the coherent length just after absorption of a photon as follows. When $T_F \ll T_D < T_L$ holds, almost a complete exciton state is produced. This case will correspond to the exciton state of B850 at low temperature. Indeed, by the single molecule spectroscopy of B850 at 1.2 K, the complete exciton state was observed in the action spectra of fluorescence.[40−42] When $T_F \sim T_D < T_L$ holds, a finite exciton coherent domain is produced. When $T_D \ll T_F < T_L$ or $T_D \ll T_L < T_F$ holds, almost a localized excited state is produced. Once the complete exciton state or exciton coherent domain is produced, its coherent length becomes gradually smaller due to the perturbation by the electron−phonon interaction and finally reaches a constant value in the steady state. Such time course of the coherent length was analyzed in detail for B850 before.[21,39] Extending this consideration, we can say that the exciton coherent domain at the time when fluorescence takes place is a much shrinked one corresponding to the one of steady state because usually fluorescence takes place in the order of nanoseconds after photoabsorption. This result is quite favorable to explain why the superradiance is so small as about 3 in B850.[20] On the basis of the above consideration, we conclude that the most extended exciton domain state or complete exciton state is observed by optical absorption while the most shrinked exciton domain state is observed by luminescence.

On the other hand, if only one molecule in the whole system is initially excited, the initial coherent length is small and it increases with time until the coherent length in the steady state. Such a thing happens in the excitation transfer from B800 to B850. In this EET, the locally excited state of B800 is initially produced and its excitation energy is transferred through the window of the nearest molecules in B850 from the locally excited B800 molecule. Before the excited energy of B800 arriving at the B850 systems, the coherent exciton state which extends over the whole B850 system is not formed because the optically mixed state is not provided to B850 initially. Therefore, the excited-state population in B850 increases gradually by the income from B800 and the coherent domain extends gradually until the value of the steady state. Such behavior was numerically solved by us recently and the result will be published elsewhere.[43]

6. Conclusion

The most important result in the present study is that we have for the first time derived an empirical formula of coherence length N_{coh} as a linear function of $\xi(\equiv 2U/\gamma)$. In the presence of the inhomogeneity, the average coherence length $\bar{N}_{coh}$ deviates a little from the linear dependence of ξ. Qualitatively, we have also shown that this empirical relation is obtained by the balance of the coherent bond-formation force U and the coherent bond-destruction force γ. To obtain this formula quantitatively, we first implemented a theoretical scheme that we solve the GME with the memory function which was derived by the second-order perturbation of the intermolecular interaction. In the

second, we implemented a new method for evaluating the coherence length by calculating the degree of coherency for each molecule, in which we adopted a physical picture developed in the dimer theory for the intermediate coupling case. Applying this formula of the coherence length to B850, we obtained N_{coh} is around 5 in the absence of inhomogeneity and around 4 in the presence of inhomogeneity. This calculated result is qualitatively in agreement with the other calculated results based on the Redfield theory.[21,39] Our theory starts from the weaker coupling case but gives a correct result in the strong coupling limit. In contrast to this, the Redfield theory is suitable to a rather stronger coupling case. The agreement of the results obtained by the two different approaches is quite significant. Our theoretical method can be used complementarily or comparatively with the other theoretical calculations.

Acknowledgment. The authors acknowledge Professor H. Sumi in Tsukuba University for valuable discussions. This work was supported by the Grant-in-Aid on Scientific Research on Priority Areas "Molecular Physical Chemistry" No. 11166230 to T.K. from the Japanese Ministry of Education, Science, Sports and Culture, and by "Research and Development Applying Advanced Computational Science and Technology" of Japan Science and Technology Corporation.

References and Notes

(1) Van Aeronger, H.; Valkunas, L.; Van Grondelle, R. *Photosynthetic Excitons*; World Scientific: Singapore, 2000.
(2) Renger, T.; May, V.; Kühn, O. *Phys. Rep.* **2001**, *343*, 137.
(3) Kühlbrandt, W.; Wang, D. N.; Fujiyoshi, Y. *Nature* **1994**, *367*, 614.
(4) Karrasch, S.; Bullough, P. A.; Ghosh, R. *EMBO J.* **1995**, *14*, 631.
(5) McDermott, G.; Prince, S. M.; Freer, A. A. Hawthornthwalte-Lawless, A. M.; Papiz, M. Z.; Cogdell, R. J.; Isaacs, N. W. *Nature* **1995**, *374*, 514.
(6) Koepke, J.; Hu, X.; Muenke, C.; Schulten, K.; Michel, H. *Structure* **1996**, *4*, 581.
(7) Hoffman, E.; Wrench, P. M.; Shaples, F. P.; Hiller, R. G.; Welte, W.; Drederichs, S. *Science* **1996**, *272*, 1788.
(8) Schubert, W. D.; Klukas, O.; Saenger, W.; Witt, H. T.; Fromme, P.; Krauss, N. *J. Mol. Biol.* **1988**, *280*, 297.
(9) Zouni, A.; Witt, H. T.; Kern, J.; Fromme, P.; Krauss, N.; Saenger, W.; Orth, P. *Nature* **2001**, *409*, 739.
(10) Sundström, V.; Pulleris, T.; van Grondelle, R. *J. Phys. Chem. B* **1999**, *103*, 2327.
(11) Sauer, K.; Cogdell, R. J.; Prince, S. M.; Freer, A.; Isaacs, N. W.; Scheer, H. *Photochem. Photobiol.* **1996**, *64*, 564.
(12) Hu, X.; Ritz, T.; Damjanović, A.; Schulten, K. *J. Phys. Chem. B* **1997**, *101*, 3854.
(13) Pullerits, T.; Sundström, V. *Acc. Chem. Res.* **1996**, *29*, 381.
(14) Hu, X.; Schulten, K. *Phys. Today* **1997**, August 28.
(15) Mukai, K.; Abe, S.; Sumi, H. *J. Phys. Chem. B* **1999**, *103*, 6096.
(16) Scholes, G. D.; Fleming, G. R. *J. Phys. Chem. B* **2000**, *104*, 1854.
(17) Jimenez, R.; Dikshit, N.; Bradforth, S. E.; Fleming, G. R. *J. Phys. Chem.* **1996**, *100*, 6825.
(18) Chacisvilis, M.; Kühn, O.; Pullerits, T.; Sundström, V. *J. Phys. Chem. B* **1997**, *101*, 7275.
(19) Novoderezhkin, V.; Monshouwer, R.; van Grondelle, R. *Biophys. J.* **1999**, *77*, 666.
(20) Monshouwer, R.; Abrahamsson, M.; van Mourik, F.; van Grondelle, R. *J. Phys. Chem. B* **1997**, *101*, 7241.
(21) Kühn, O.; Sundström, V. *J. Chem. Phys.* **1997**, *107*, 4154.
(22) Redfield, A. G. *Adv. Magn. Reson.* **1965**, *1*, 1.
(23) Ray, J.; Makri, N. *J. Phys. Chem. A* **1999**, *103*, 9417.
(24) Jimenez, R.; van Mourik, F.; Yu, J. Y.; Fleming, G. R. *J. Phys. Chem.* **1997**, *101*, 7350.
(25) Meier, T.; Chernyak, V.; Mukamel, S. *J. Phys. Chem. B* **1997**, *101*, 7372.
(26) Zhao, Y.; Meier, T.; Zhang, W. M.; Chernyak, V.; Mukamel, S. *J. Phys. Chem. B* **1999**, *103*, 3954.
(27) Kakitani, T.; Kimura, A.; Sumi, H. *J. Phys. Chem. B* **1999**, *103*, 3720.
(28) Kimura, A.; Kakitani, T.; Yamato, T. *J. Phys. Chem. B* **2000**, *104*, 9276.
(29) Förster, Th. In *Modern Quantum Chemistry, Part III*; Sinanolglu, O., Ed.; Academic Press: New York, 1965; p 93.
(30) Förster, Th. *Discuss. Faraday Soc.* **1959**, *27*, 7.
(31) Kimura, A.; Kakitani, T. Manuscript in preparation.
(32) Kenkre, V. M.; Knox, R. S. *Phys. Rev.* **1974**, *B9*, 5279.
(33) Mukamel, S.; Franchi, D. S.; Loring, R. F. *Chem. Phys.* **1988**, *128*, 99.
(34) Jean, J. M.; Friesner, R. A.; Freming, G. R. *J. Chem. Phys.* **1992**, *96*, 5827.
(35) Jean, J. M.; Freming, G. R. *J. Chem. Phys.* **1995**, *103*, 2092.
(36) Leegwater, J. A. *J. Phys. Chem.* **1996**, *100*, 14403.
(37) Kühn, O.; Sundström, V. *J. Phys. Chem. B* **1997**, *101*, 3432.
(38) Meier, T.; Zhao, Y.; Chernyak, V.; Mukamel, S. *J. Chem. Phys.* **1997**, *107*, 3876.
(39) Dahlbom, M.; Pullerits, T.; Mukamel, S.; Sundström, V. *J. Phys. Chem. B* **2001**, *105*, 5515.
(40) van Oijen, A. M.; Ketelaars, M.; Köhler, J.; Aartsma, T. J.; Schmidt, J. *Science* **1999**, *285*, 400.
(41) Ketelaars, M.; van Oijen, A. M.; Matsushita, M.; Köhler, J.; Schmidt, J.; Aartsma, T. J. *Biophys. J.* **2001**, *80*, 1591.
(42) Matsushita, M.; Ketelaars, M.; van Oijen, A. M.; Köhler, J.; Aartsma, T. J.; Schmidt, J. *Biophys. J.* **2001**, *80*, 1604.
(43) Kimura, A.; Kakitani, T. Manuscript in preparation.